Hindawi
Advances in Civil Engineering
Volume 2023, Article ID 6692746, 15 pages
https://doi.org/10.1155/2023/6692746

Research Article

Fuzzy Comprehensive Evaluation Method for Evaluating Stability of Loess Slopes

Xiaopeng Deng and Xinghua Xiang

Shanxi Institute of Energy, No. 63 University Street, University Park, Jinzhong 030600, Shanxi, China

Correspondence should be addressed to Xinghua Xiang; xiangxh@sxie.edu.cn

Received 11 May 2023; Revised 19 October 2023; Accepted 25 October 2023; Published 23 November 2023

Academic Editor: Panpan Xu

Copyright © 2023 Xiaopeng Deng and Xinghua Xiang. This is an open access article distributed under the Creative Commons Attribution License, which permits unrestricted use, distribution, and reproduction in any medium, provided the original work is properly cited.

The stability assessment of loess slopes is of great significance for slope reinforcement and safety assessment. This research studies the main factors affecting the stability of the loess slope through the summary and analyzes the failure cases of the loess slope in Shaanxi Province. The importance of influencing factors was studied through numerical simulation method, sensitivity analysis method, and gray correlation analysis method, and the weight value method was given. On this basis, we have developed the fuzzy comprehensive evaluation model method for assessing the stability of loess slopes based on the principle of maximum membership degree. Finally, the method was applied to the stability analysis of the actual loess slope, and the rationality and correctness of the loess slope stability evaluation method proposed in this paper were demonstrated. The results showed that, for the Shaanxi loess slope, the probability of instability of the positive slopes is far greater than that of negative slopes; the greater the slope gradient, the more unstable the loess slopes. Collapse mainly occurs in the range of 10–40 m slope height. There is a significant positive correlation between rainfall and the probability of loess landslides. The degree of correlation between the factors influencing slope stability and the safety factor can be categorized from strong to weak as follows: slope inclination > internal friction angle > height of the slope > gravitational forces > cohesion > Poisson’s ratio > modulus of elasticity, and the influence of Poisson’s ratio and elastic modulus can be ignored. The fuzzy comprehensive evaluation method based on the gray correlation degree method established in this paper was used to evaluate the stability of the loess slopes. The evaluation results attested to the actual data of slope monitoring. The evaluation method proves reasonable and feasible and can be well applied to the stability analysis of the loess slopes.

1. Introduction

Landslide disaster occurs almost all over the world in mountainous areas with human living and engineering activities. It has become one of the most common geological disasters at present and has caused great losses. China is the region with the most severe landslides in Asia and even the world, while northern Shaanxi, Gansu, Shanxi, and other regions covered by loess are the provinces that suffer from more serious landslide geological disasters in China. As the type of geological disaster with the highest frequency and the largest loss at home and abroad, especially in the loess regions, landslide geological disasters seriously endanger social development and people’s safety [1–5]. It is obviously of great significance to clarify the factors affecting the stability of the loess slopes and to conduct reasonable stability analysis and evaluation of the loess slopes.

The failure mode of a high loess slope is an essential basis for understanding the mechanism of slope disaster. Also, many other factors affect the failure mode of a high loess slope. Zhuang et al. [6] used flume and triaxial tests to study clay content’s influence on the loess slope’s failure process. The results showed that the clay content in loess significantly impacts the failure process and strength of the loess body. Li et al. [7] studied the macropore structure of loess by X-ray computed tomography. The results showed that the permeability of loess in the vertical direction is higher than that in the horizontal direction, which is easy to cause excessive permeability and preferential flow, thus causing the instability of the loess slopes; large pores lead to considerable water permeability, which is easy to induce instability of the loess slopes. The influence of loess permeability on mechanical properties was investigated by Xu et al. [8, 9], who conducted a series of tests, including permeability tests, scanning electron microscope tests, and leaching tests. The research showed that loess permeability mainly affects its mechanical properties by changing the microstructure of soil. Xu et al. [10] studied the influence of dry–wet cycles on the mechanical properties, crack development, and failure mode of loess under uniaxial compression using laboratory test method. Zhuang et al. [1, 11] studied the impact of rainfall on loess landslides by means of field investigation and monitoring, in situ testing, laboratory test, and numerical calculation. The results showed that the loess slopes are particularly sensitive to long-term heavy rainfall, and the early rainfall played an important role in triggering loess landslides. The rain-induced landslides were mainly caused by the loess's loose and highly porous structure. Xu et al. [12] studied the impact of freeze-thaw cycles on the failure modes of loess landslides through field investigation, monitoring, and model test. The findings of the study indicated that freeze-thaw cycles contribute significantly to landslide failure through erosion, spalling, and thawing mechanisms. Moreover, the primary cause of freeze-thaw-induced landslide failure can be attributed to the high porosity and loose cementation structure characteristic of loess. Hao et al. [13] used the indoor soil test method to clarify the macrobehavior and micromechanism about the impact of bound water on the shear strength of loess. The research showed that the bound water in loess can change the soil microstructure, resulting in a negative correlation between the water content of bound water and the shear strength. Hou et al. [14] used indoor one-dimensional column test and two-dimensional numerical simulation method to study the infiltration characteristics of loess. The results showed that the existence of hydraulic gradient significantly impacts the infiltration characteristics of loess, and controlling or reducing irrigation water is a feasible means to control loess landslides. Chang et al. [15] used the discrete element method to study the influence of joint shape on the failure rule of loess slopes. The results indicated that the failure mode of loess slopes with joints is, first, cracks propagate along both ends of the joints; then, the sliding body slides along the joint surface. Wu et al. [16] used the shaking table test method to study the dynamic response characteristics and deformation and instability rules of loess slope under an earthquake. The results showed that the failure modes of the fractured slope are crack development, crack expansion, soil collapse at the slope shoulder, shear failure at the high side of the slope, shear failure at the low side of the slope, and formation of new cracks at the edge of the platform. Zhang et al. [17] discussed the characteristics and prevention mechanism of the loess slope instability by field investigation and the backpropagation neural network (BPNN) method. The results showed that the difference in soil moisture content and failure modes leads to a significantly higher degree of instability for the shady slopes and the downhill slopes than that for the sunny slopes and the upslopes; slope gradient, soil compaction, slope height, and soil shear strength have significant effects on slope instability. The existing research results on factors affecting the stability of the loess slopes showed that the loess's loose and highly porous structure are the internal factors affecting the stability of the loess slopes, while water is the extremely important external factor affecting the stability of the loess slopes.

The slope stability evaluation informations are incomplete, multiple, and uncertain. The stability evaluation of the loess slopes has always been challenging for scholars. The slope is a complex, dynamic system with uncertainty (fuzziness, randomness, incomplete information), nonlinearity, and heterogeneity. At present, slope stability analysis methods can be roughly divided into two categories, namely qualitative analysis methods and quantitative analysis methods. The qualitative analysis methods are mainly based on accumulating geological information and engineering experience, considering the slope's development environment and essential characteristics. It is used to analyze the cause of the formation and evolution history of the historical deformation geological body and the mechanical mode of slope instability. The most significant advantage of this qualitative slope stability evaluation methods is that it can comprehensively consider various indicators that affect the slope stability and then quickly evaluate the slope's current stability and future development trend. Meanwhile, it is evident that these approaches also have their limitations. They necessitate engineers to possess extensive practical expertise, encounter numerous unpredictable variables, exhibit excessive subjectivity, and lack standardized evaluation criteria [18, 19]. Quantitative analysis methods mainly include deterministic analysis methods and uncertainty analysis methods. The rigid body limit equilibrium analysis methods and numerical analysis methods are the most commonly used deterministic analysis methods. The limit equilibrium analysis methods mainly refer to various slice methods [20, 21]. The numerical analysis methods mainly include the finite element method [22], the boundary element method [23], the finite difference method [24], the discrete element method [25], and various machine learning methods [26–28]. Uncertainty analysis methods mainly include probability analysis method [29], information quantity model method [30], reliability analysis method [31], gray system evaluation method [32], fuzzy comprehensive evaluation method [33], other uncertainty analysis methods, and composite methods.

The nature of loess is different from that of ordinary soil, which directly leads to the complexity of the stability analysis for loess slopes and the inability to use the stability analysis methods of the ordinary slope directly. There are many factors that affect slope stability, and the stability analysis of loess slopes is a relatively complex system engineering. The gray correlation analysis method has no requirement for the required sample size, is simple to calculate, and the results are consistent with the qualitative results [34, 35]. The fuzzy comprehensive evaluation method uses precise digital means to process fuzzy evaluation objects, and can make a more scientific, reasonable, and practical quantitative evaluation of data containing fuzzy information [36, 37]. This paper

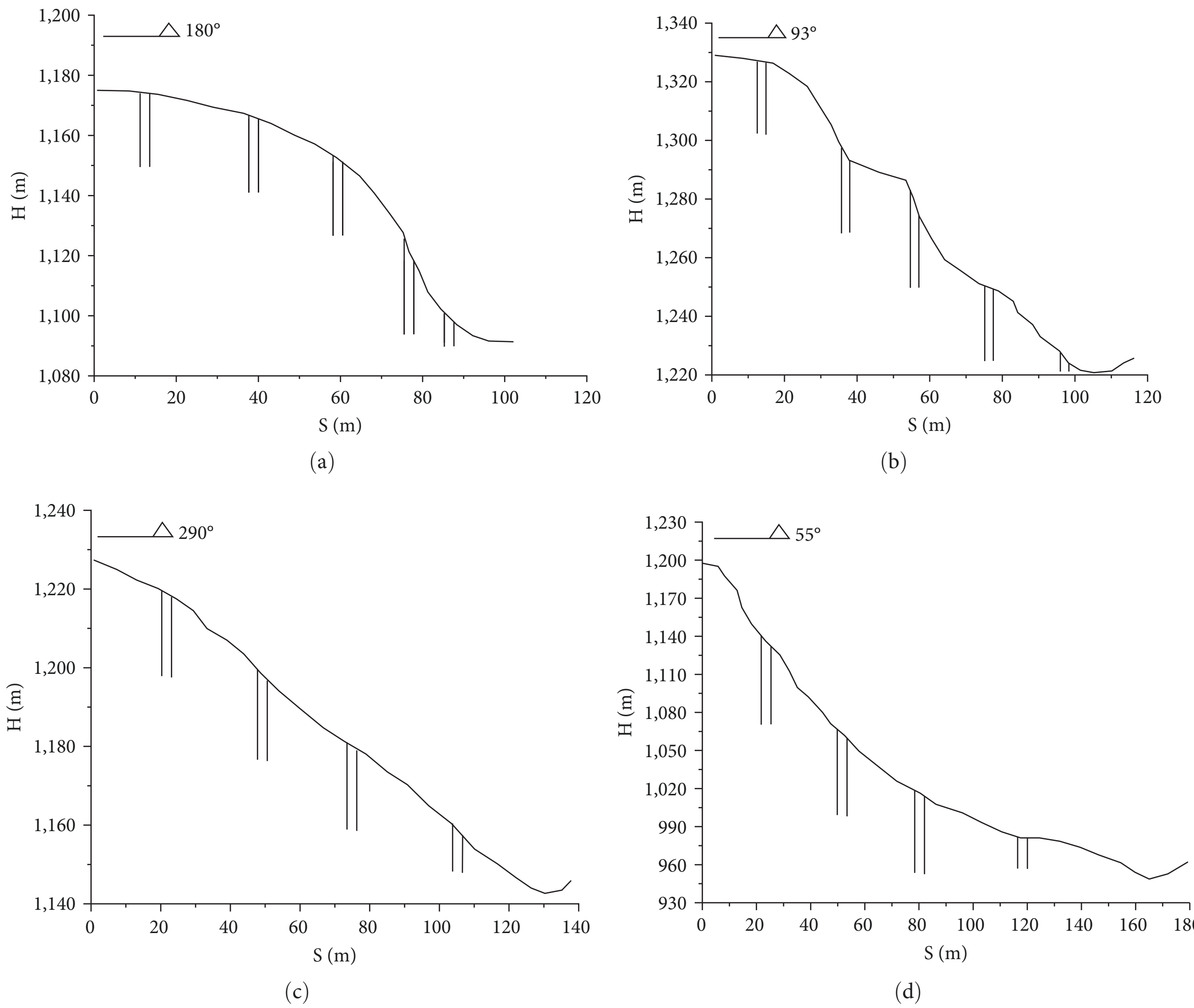

Figure 1: Schematic diagram of loess slope shapes: (a) convex shape; (b) stepped shape; (c) straight shape; (d) concave shape.

attempts to introduce these two methods into the stability analysis of loess slopes. The Shaanxi loess slope was taken as the research object in this paper. First, geological survey and statistical analysis determined the influence factors of loess slope stability. Then, combined with the results of multivariable finite element numerical calculation and the gray correlation method [38, 39], the classification standard of loess slope stability was obtained, and the fuzzy comprehensive evaluation model of loess slope stability was established using the principle of maximum membership degree [40]. Finally, the fuzzy comprehensive evaluation model for assessing the stability of loess slopes was implemented in practical engineering, subsequently validated and compared against real-time slope monitoring data.

2. Statistics of Influencing Factors for Loess Slope Stability

Based on the previous studies, the geological data of 403 typical road slopes in Baota District in Yan'an City, Linyou County in Shaanxi Province, and Qinba Mountain in Shaanxi Province were collected and sorted out. The 403 landslides survey data were used as samples for statistical analysis to analyze the impact of slope shape, slope gradient, slope height, and rainfall on the stability of the loess slopes. All 403 slopes were ever damaged by landslides or collapse.

2.1. Slope Shape. A loess slope is a typical soil slope. The slope type of loess is mainly divided into two categories: positive landslide (i.e., dip slope) and negative landslide (i.e., reverse slope). These two categories are subdivided into four categories according to the slope shape: convex, stepped, straight, and concave, as shown in Figure 1(a)–1(d). The 403 typical slopes are classified according to different slope types, and the results are shown in Table 1.

There are 303 straight and convex landslides of the positive type and 100 concaves and stepped landslides of the negative type. The proportion of positive landslides is 75%, and that of negative landslides is 25%. The specific distribution of the four slope shapes is shown in Table 1. From the

Table 1: Quantity distribution of landslides with different slope shapes.

Slope shape (before failure)	Convex shape	Concave shape	Stepped shape	Straight shape
Linyou	10	19	48	8
Baota	107	10	21	154
Qinba	16	1	1	8

Table 2: Distribution of landslides with different slope gradients.

Slope gradient	10°–25°	25°–35°	35°–45°	45°–60°	60°–90°	Total
Linyou	23	25	29	6	2	85
Baota	0	141	94	54	4	292
Qinba	1	7	11	4	3	26
Total	23	173	134	62	9	403
Percentage (%)	6	43	33	16	2	100

Table 3: Quantity distribution of landslides with different slope heights.

Slope height (m)	<10	10–20	20–30	30–40	40–50	50–60	60–70
Number of landslides	2	3	11	10	10	5	13
Percentage (%)	2.4	3.5	12.8	11.8	11.8	5.9	15.2
Slope height (m)	70–80	80–90	90–100	100–120	120–140	140–160	>160
Number of landslides	4	9	5	5	6	2	0
Percentage (%)	4.7	10.6	5.9	5.9	7.1	2.4	0

analysis of the quantity distribution table of different slope shapes, it can be seen that the number of positive landslides is far greater than that of negative landslides, whereas the number of the concave slope is the smallest, and the number of convex and straight landslide is more. According to the analysis of the stress distribution of slopes with different slope shapes, it can be seen that the concave and stepped slopes tend to reduce the dead load along the slope direction, and the degree of stability is significantly greater than that of the positive slope, and the number of landslide disasters for the positive slopes is big. The probability of a positive slope instability is far greater than that of a negative slope.

2.2. Slope Gradient. The slope gradient of the loess slope is an important index that affects slope stability. The slope gradient determines the stress distribution of the slope, and the slope size directly affects the formation of surface runoff on the slope surface, the change of groundwater level inside the slope, and the growth of vegetation on the slope surface after rainfall. According to the slope distribution of 403 typical slopes, the number of landslides with different slope gradients is divided into six sections: 0°–10°, 10°–25°, 25°–35°, 35°–45°, 45°–60°, 60°–90°, and then the number of landslides with different slope gradients is counted. The statistical results are shown in Table 2. The number of landslides in the statistical area is the largest when the slope gradient is 25°–35° and 35°–45°, accounting for 76.6%. When the slope gradient is 45°–60°, the number of landslides is also significant, and in other slope gradient ranges, the number of landslides is small. The statistical results show that there are basically no landslides in the study area when the slope gradient is 0°–10°. According to the statistical results, the number of landslides with a slope gradient of 25°–45° is significantly greater than that of other slope gradient ranges, but for this statistical result, it cannot be simply agreed that the probability of landslides with a slope gradient of 25°–45° must be the largest. Taking the statistical data of Baota District in Yan'an City as an example, the number of landslides with a slope gradient of 25°–35° is 141, and the number of landslides with a slope gradient of 60°–90° is only four. From the data can it be seen that the number of landslides is less when the slope gradient is large. However, the probability of landslide occurrence under different slope gradients is not simply a comparison of the specific number of landslides under different gradients. The correct meaning of the probability for landslide occurrence is to divide the number of landslides in a section of slope gradient by the number of all slopes in the area. Generally speaking, under the same conditions, the larger the slope gradient, the more unstable the slope is and the more prone to landslides.

2.3. Slope Height. Slope height is also an important factor in slope stability. The statistical results of the original slope height of the landslides in Linyou County (from 1960 to 2004) are shown in Table 3, and the statistics of the number of collapses at different slope heights are shown in Table 4.

The statistical results showed that landslides mainly occur in the range of 20–70 m, with 49 landslides accounting for 57.6% of the total number. Second, in the range of 70–140 m, there are 29 landslides, accounting for 24.1% of the total number. In the range of slope height >140 m, there are two landslides, accounting for 2.35% of the total number.

Table 4: Quantity distribution of collapses at different slope heights.

Slope height (m)	<10	10–20	20–30	30–40	40–50	>50
Number of collapses	8	19	6	3	0	3
Percentage (%)	20.5	48.7	15.4	7.7	0	7.7

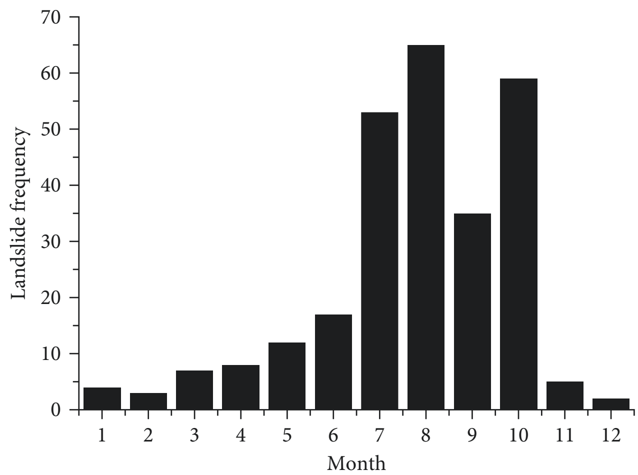

Figure 2: Statistics for the number of loess landslides in the study area every month from 1960 to 2004.

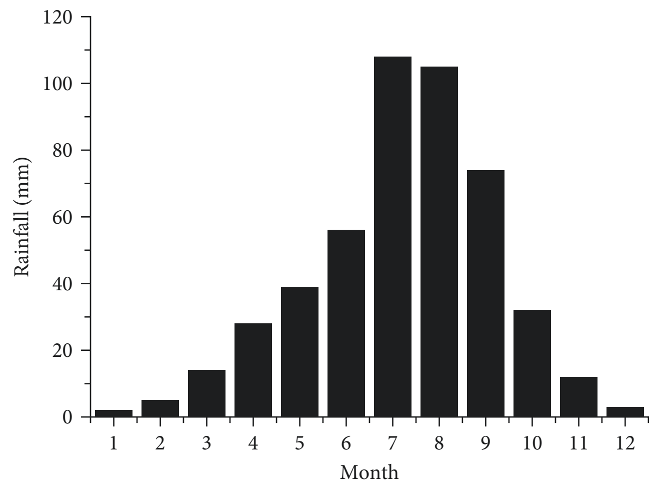

Figure 3: Monthly rainfall statistics of the study area from 1960 to 2004.

There are five landslides within the range of slope height <20 m, accounting for 5.9% of the total number.

Most of the collapses occur on steep cliffs with a slope height of 10–30 m, with 25 collapses accounting for 64.1% of the total collapses. Second, it occurs on a steep cliff with a slope height of less than 10 m, with eight collapses, accounting for 20.5% of the total number. The slope height is more than 30 m, and the collapse occurs only six times, accounting for 15.4% of the total collapse. It can be seen that the slope height of 20–60 m is the high-risk range of landslides, the slope height of 60–120 m is the medium-risk range of landslides, the slope height of less than 20 m and more than 120 m is the low-risk range of landslides, and collapse mainly occurs in the range of 10–40 m slope height. The main reason is that as the height of the slope increases, the weathering and erosion time it experiences become longer. During this process, the slope gradually slows down, and under certain induced conditions, landslides occur or the slope gradually decreases and tends to stabilize; the lower the height of the slope, the greater the possibility of forming a steep slope, and it has a higher probability of collapse caused by factors such as river erosion, rainfall, or human activities.

2.4. Rainfall. The loess landslides in the study area mainly occurred in Baota District, Ganquan County, Fuxian County, Huangling County, and other places in Yan'an City. According to the statistics of geological disasters from 1960 to 2004, there was a high rainfall in the region in 2003. There was a long period of heavy rainfall in the year, and loess landslides frequently occurred during the rainfall period. Figure 2 shows the statistics for the number of loess landslides from 1960 to 2004 monthly. The statistical results showed that the number of loess landslides in the rainy season from July to October is significantly higher than that in other months, especially in August when the number of loess landslides reaches the maximum, and there is an obvious high incidence.

The meteorological rainfall data from 1960 to 2004 were statistically analyzed, as shown in Figure 3. The meteorological data showed that the annual rainfall in the study area is extremely uneven. There is very little rainfall in winter from November to March of the following years. After May, the rainfall begins to increase gradually. In the rainy season, the rainfall from July to September reaches the maximum, accounting for more than 60% of the annual rainfall.

If the monthly landslide times were compared with the monthly regional rainfall, it can be seen that the annual rainfall distribution in the study area is extremely uneven. There is little rainfall during winter from November to March of the following year. After May, rainfall increases gradually, reaching the maximum in the rainy season from July to September. At the same time, in the corresponding month, the number of landslides begins to increase from May, which coincides with the time when the rainfall began to increase. The number of loess landslides also reached the maximum value from July to September, when the rainfall was the largest. There is a special case that the number of loess landslides in October is more than that in September. This is because, in October 2003, Huangling County in the study area experienced a long period of heavy rainfall, which caused many landslide geological disasters in Huangling County. By comparing the average monthly rainfall and the number of loess landslides in the corresponding month, it can be found that there is a significant positive correlation between the two. With large rainfall in July, August, September, and October, loess landslides occur frequently, showing a high incidence.

3. Evaluation Method of Loess Slope Stability

The slope is a nonlinear and uncertain dynamic system affected by many factors. Many field tests, laboratory tests, and engineering construction problems showed that slope stability is a thing without clear boundaries. The stability of the slopes cannot be defined simply by a numerical value. There is no clear and accurate definition for the stability and instability of slope, which has great ambiguity.

Based on the theory of fuzzy mathematics, the fuzzy comprehensive evaluation method established by the fuzzy set [41] can integrate multiple indicators to evaluate the evaluation object. This method divides the scope of the object to evaluate it. On one hand, it can fully reflect the fuzziness of the object to be evaluated and make the evaluation standard more reasonable; on the other hand, people's experience can be fully used in the evaluation process to make the evaluation results more objective and consistent with the actual situation.

The weight distribution of evaluation indicators directly affects the accuracy of the evaluation results, so determining the weight of the evaluation indicators is an extremely important part of the fuzzy comprehensive evaluation method. The weight distribution must wholly and correctly reflect the importance of each evaluation indicator. There are 3 main methods for the weight distribution of evaluation indicators: expert consultation method (Delphi method), expert survey method, and analytic hierarchy process. The expert consultation method and survey method are relatively simple, but subjective human factors greatly impact the evaluation results. The analytic hierarchy process is to gradually compare the importance of various relevant factors and use less quantitative information to informatization the decision-making process. Compared with expert consultation method and survey method, the analytic hierarchy process has lower subjective factors, but it also needs to rely on expert scoring in determining the weight, which is too subjective. Therefore, this paper introduces the gray correlation degree method into the weight determination of the loess slope stability evaluation and determines the weight value of each index through the sensitivity analysis of the evaluation index based on the gray correlation degree method, which can overcome the problem that the former methods are too subjective and obtain better results. Therefore, this paper used the fuzzy comprehensive evaluation method based on the gray correlation degree method to evaluate the stability of the loess slopes.

3.1. Basic Theory of Fuzzy Comprehensive Evaluation Method. The comprehensive evaluation method based on fuzzy theory considers the influence of various factors simultaneously and comprehensively evaluates the evaluation object. When the evaluation object has typical fuzziness, the fuzzy comprehensive evaluation method can often obtain better results. The stability evaluation of highway slopes in the loess area is obviously quite fuzzy, so it is very suitable to use a fuzzy comprehensive evaluation to evaluate the slope stability and can obtain more objective and accurate evaluation results.

3.1.1. Basic Theory. There are two domains: factor set $U = \{u_1, u_2, \cdots, u_n\}$ (u_i is the evaluation factor) and evaluation set $V = \{v_1, v_2, \cdots, v_m\}$ (v_j is the evaluation level). If each element u_i in U is operated separately $f(u_i)$, it can be regarded as a fuzzy mapping from U to V, and the fuzzy matrix R can be derived from the fuzzy mapping f as follows:

$$\mathbf{R} = \left(r_{ij}\right)_{n\times m}, 0 \leqslant r_{ij} \leqslant 1, \tag{1}$$

where R is the single factor evaluation matrix from U to V. If there is a fuzzy subset $A = \{a_1, a_2, \cdots, a_n\}$ on the set U, A is expressed as a vector and satisfies as follows:

$$\sum_{i=1}^{n} a_i = 1, \tag{2}$$

where a_i is the weight of the ith factor, which can uniquely determine the fuzzy transformation B from U to V, and B is the result of fuzzy synthesis.

$$B = A \cdot R. \tag{3}$$

Note $B = \{b_1, b_2, \cdots, b_m\}$, where b_j reflects the membership of the jth evaluation v_j and fuzzy set B. According to the principle of maximum membership, select the largest $\max\{b_1, b_2, \cdots, b_m\}$ from B, and the corresponding grade is the final result of the fuzzy comprehensive evaluation.

The membership function describes fuzzy sets and is the basis of the whole fuzzy theory. Therefore, it is very important to establish a membership function that conforms to the objective laws of the things to be evaluated. Statistical method and subset comparison method are usually used to determine the membership function. The representation method of the membership function can be divided into the discrete type and continuous type. Generally, their membership can be assigned based on experience for discrete indicators. For continuous indicators, the appropriate distribution form can be selected according to the characteristics of the indicators. The commonly used fuzzy distributions include trapezoid, triangle, normal, bell, k-degree parabola, etc. Each type of distribution can be divided into three types: the upper type, the central type, and the lower type.

3.2. Basic Theory of Gray Correlation Method. The gray correlation analysis method is an important part of the gray system theory. It is a method to quantify the degree of mutual influence between various factors or determine the contribution of several subfactors to the main factors. This method can use fewer data to accurately find the correlation between each evaluation index and the evaluation object, and the correlation size is quantified by a gray correlation degree. The greater the correlation degree, the more obvious the impact of the evaluation index on the evaluation object and the stronger the correlation.

First, the sequence data of each subfactor are processed to make the sequence have accessibility, comparability, and polarity consistency to obtain the gray correlation factor space. Then, through the difference information between the sequences, the difference information space is established, and the difference information comparison measure, namely the gray correlation degree, is calculated. Finally, the gray correlation degree from large to small is ranked, and the influence of each subfactor on the reference factor is analyzed. The specific steps are:

(1) Determine the reference sequence matri

The influence factors of loess slope stability (such as gravity, cohesion, internal friction angle, seismic acceleration, etc.) are selected as subsequence X, namely:

$$X = \begin{bmatrix} X_1 \\ X_2 \\ \vdots \\ X_4 \end{bmatrix} = \begin{bmatrix} x_{11} & x_{12} & \cdots & x_{1j} \\ x_{21} & x_{22} & \cdots & x_{2j} \\ \vdots & \vdots & \ddots & \vdots \\ x_{i1} & x_{i2} & \cdots & x_{ij} \end{bmatrix}. \tag{4}$$

The slope stability coefficient K under the corresponding conditions of each subsequence factor is selected as the parent sequence Y. The stability coefficient is calculated by the corresponding calculation method, and its matrix can be expressed as follows:

$$Y = \begin{bmatrix} Y_1 \\ Y_2 \\ \vdots \\ Y_4 \end{bmatrix} = \begin{bmatrix} y_{11} & y_{12} & \cdots & y_{1j} \\ y_{21} & y_{22} & \cdots & y_{2j} \\ \vdots & \vdots & \ddots & \vdots \\ y_{i1} & y_{i2} & \cdots & y_{ij} \end{bmatrix}, \tag{5}$$

where x_{ij} represents the change value of the ith factor, y_{ij} is the value of the jth stability coefficient corresponding to the change of the ith factor, i is the number of factors considered, and j represents the number of stability coefficient values corresponding to the change of the ith factor.

(2) Range change of sequence factor

As the dimension of each factor is different, and the values are very different, it is necessary to process the data of each factor to eliminate the influence of the dimension for each factor in the parent sequence and subsequence. Here, the method of range change is used for processing, namely:

$$x'_{ij} = \frac{x_{ij} - \min x_{ij}}{\max x_{ij} - \min x_{ij}}, \tag{6}$$

$$y'_{ij} = \frac{y_{ij} - \min y_{ij}}{\max y_{ij} - \min y_{ij}}, \tag{7}$$

where x'_{ij} is the normalized value corresponding to x_{ij}, and y'_{ij} is the normalized value corresponding to y_{ij}.

Make the following changes from the processed child and parent sequences to form a new difference sequence matrix Δ:

$$\Delta_{ij} = \left| x'_{ij} - y'_{ij} \right|. \tag{8}$$

Take the maximum and minimum values in the new sequence, namely:

$$\Delta_{\max} = \max \Delta_{ij}, \tag{9}$$

$$\Delta_{\min} = \min \Delta_{ij}. \tag{10}$$

(3) Calculation of correlation coefficient matrix and correlation degree

The elements in the correlation coefficient matrix L are as follows:

$$l_{ij} = \frac{\Delta_{\min} + \eta \Delta_{\max}}{\Delta_{ij} + \eta \Delta_{\max}}, \tag{11}$$

where η is the resolution coefficient, which is used to improve the significance of the difference between the correlation coefficients, generally $\eta = 0.5$. As a measure of the similarity for the index sequence, the correlation degree is the amount of change within the interval $[0, 1]$, and the closer the correlation degree is to 1, the more sensitive the influence of the subsequence on the parent sequence is; on the contrary, the closer the correlation degree is to 0, the less sensitive its impact is. The calculation of the correlation degree g_i can be obtained from the following formula as follows:

$$g_i = \frac{1}{n} \sum_{j=1}^{n} l_{ij}. \tag{12}$$

In the formula, n is the number of influencing factors considered when calculating the correlation degree.

(4) Sensitivity evaluation and weight distribution

Rank the correlation degree g_i from the largest to the smallest. The greater the correlation degree, the more sensitive the factor is the slope stability according to the maximum correlation degree identification principle. Finally, the correlation degree g_i is normalized to obtain the weight of each factor.

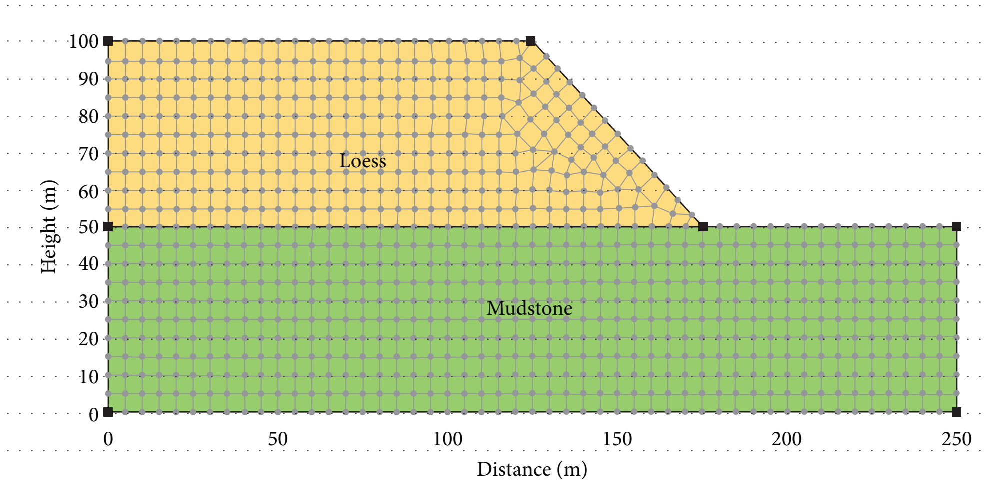

FIGURE 4: Benchmark model of slope finite element calculation.

3.3. Selection of Evaluation Indicators Based on Sensitivity Analysis

3.3.1. Preliminary Selection of Evaluation Indicators. The establishment of the evaluation index system is a very difficult task. There is no uniform criterion for selecting the index system, which often depends on expert experience and historical statistical data. The rationality of slope stability evaluation results largely depends on the reliability and accuracy of evaluation indicators, which should fully reflect the basic conditions of the slope under study. The evaluation index system of slope stability shall meet the following principles:

(1) Systematic principle. Slope stability evaluation is a systematic project with many complex influencing factors. The selected evaluation index should be systematic and comprehensive, covering all aspects affecting slope stability as far as possible.

(2) The principle of representativeness. Many factors affect slope stability, among which there are often controlling factors. When selecting evaluation indicators, the essence of the problem should be grasped, and the indicators should effectively reflect the stability of a slope.

(3) Principle of operability. The evaluation index system serves for the rapid evaluation of slope stability. Therefore, the index system should be convenient for technicians to collect relevant data during the field survey and assign values on-site as much as possible.

(4) The principle of hierarchy. The factors affecting slope stability include internal and external factors. The evaluation index system should be clear in a hierarchy and reasonable in structure, reflecting that the slope stability is affected by the joint action of internal and external factors.

Many factors affect the stability of the loess highway slope. It is necessary to clarify the relationship between each factor and the overall stability of the slope. In this paper, the evaluation index is selected based on the qualitative analysis of the factors affecting the stability of the loess highway slope. The gray correlation method analyzes the correlation between the evaluation indexes and the safety factor. Finally, the weight of the influence factors on slope stability was obtained to establish a comprehensive evaluation index system for slope stability of mountain highways. According to the systematic principle, representativeness principle, operability principle, and hierarchy principle of evaluation index selection, seven evaluation indexes, including slope height, slope angle, unit weight, cohesion, internal friction angle, elastic modulus, and Poisson's ratio, were preliminarily selected.

3.3.2. Sensitivity Analysis of Factors to Determine Evaluation Indicators. (1) Establishment of numerical model. Slope sensitivity analysis is to study the correlation between the parameters affecting slope stability and the corresponding stability coefficient. Considering the influence of slope height, slope angle, the cohesion, internal friction angle, unit weight, elastic modulus, and Poisson's ratio on slope stability, the SIGMA/W module in GeoStudio is used for stress analysis. Then, the calculation results are imported into the SLOPE/W module for limit equilibrium analysis.

The height of the high slopes in Huangyan Expressway is between 30 and 90 m, and the slope angle is between 20° and 60°. The stratum in the Huangyan Expressway area is underlain by Q2 loess with a large thickness, and the underlying stratum is completely weathered and strongly weathered argillaceous siltstone and silty mudstone. It can be seen from the previous tests that the strength of loess decreases significantly after encountering water. At the same time, the antiweathering ability of argillaceous siltstone and silty mudstone is weak, and it has the characteristics of softening when encountering water, dry cracking, and collapse after losing water, which is easy to form landslides. The slope height is 50 m, the slope angle is 45°, the cohesion of the upper rock and soil mass is 40 kPa, and the internal friction angle is 22°. In order to simplify the calculation, the calculation model is simplified into two layers, the upper layer is loess, and the lower layer is mudstone. The simplified finite element calculation base model is shown in Figure 4. The support of the

Table 5: Parameter value of finite element calculation.

Rock–soil layer	Unit weight γ (kN/m^3)	Elastic modulus E (MPa)	Poisson's ratio μ	Cohesion c (kPa)	Internal friction angle φ (°)
Upper rock and soil mass	18	30	0.3	40	22
Lower rock and soil mass	25	2000	0.2	150	40

slope model is constrained by the horizontal directions of the left and right boundaries, the horizontal and vertical directions of the bottom boundary, the other free boundary, and the load is the dead weight of the slope. The parameter values of the finite element model are shown in Table 5.

(2) Factor sensitivity analysis. As mentioned above, the slope height is 50 m, the slope angle is 45°, the cohesion of the upper rock and soil is 40 kPa, the internal friction angle is 22°, the elastic modulus is 30 MPa, and the Poisson's ratio is 0.3. SIGMA/W module in GeoStudio is used for stress analysis. Then, the calculation results are imported into the SLOPE/W module for limit equilibrium analysis, and the safety factor of the benchmark model is calculated.

The value of slope height shall be changed separately, while other parameters remain unchanged. The limit equilibrium analysis was carried out through the slope module of GeoStudio to obtain the safety coefficient corresponding to each slope height, draw the relationship curve between the safety coefficients and the slope heights (as shown in Figure 5(a)), and use the linear fitting method to fit the curve to obtain the fitting coefficient. Similarly, the safety coefficient when the slope angle, unit weight, cohesion, internal friction angle, elastic modulus, and Poisson's ratio were changed separately is shown in Figure 5(b)–5(g). It should be noted that the abscissa, as shown in in Figures 5(a) and 5(b), is dimensionless using the method of dividing by the reference for a more intuitive response sensitivity.

According to the comparison of the parameter influence fitting factors of each evaluation index, the correlation degree of each influence factor and the safety factor can be found from the largest to the smallest in order: slope angle > internal friction angle > slope height > unit weight > cohesion > Poisson's ratio > elastic modulus. The correlation degrees for Poisson's ratio and elastic modulus are 0.0726 and 0.0012, which are two orders of magnitude lower than the value of the other five evaluation indicators, and the impact degree from Poisson's ratio and elastic modulus can be ignored. Therefore, according to the sensitivity analysis of the evaluation indexes, the evaluation index factors of slope stability are determined as follows: slope height, slope angle, internal friction angle, cohesion, and unit weight.

3.4. Establishment of Slope Stability Evaluation System

3.4.1. Establishment of Evaluation Grade Standard for Loess High Slope Stability. Based on the statistics of landslide factors and the existed experimental study of loess strength characteristics in the loess area [42] and numerical analysis calculation results, the grading criteria of slope geological hazard evaluation indicators are obtained through comprehensive analysis. The basic reference conditions for each evaluation index corresponding to different stability grades are shown in Table 6.

3.4.2. Establishment of Evaluation Index Membership Function. In fuzzy mathematics, the membership degree describes the membership relationship between the object factor set and the evaluation set. According to the mathematical classification, this paper's evaluation indexes of loess slope stability (slope height, slope angle, internal friction angle, cohesion, and unit weight) are all continuous (quantitative factor). For continuous evaluation factors, the functional relationship between the membership degree and the value of the factors was established by using the commonly used "falling half trapezoid triangle rising half trapezoid" distribution, that is, the membership function.

$$U_{\mathrm{I}}(x) = \begin{cases} 1 & x \le S_1 \\ \dfrac{S_2 - x}{S_2 - S_1} & S_1 < x \le S_2, \\ 0 & x > S_2 \end{cases} \tag{13}$$

$$U_{\mathrm{II}}(x) = \begin{cases} 0 & x \le S_1 \text{ or } x > S_3 \\ -\dfrac{S_1 - x}{S_2 - S_1} & S_1 < x \le S_2 \\ \dfrac{S_3 - x}{S_3 - S_2} & S_2 < x \le S_3 \end{cases}, \tag{14}$$

$$U_{\mathrm{III}}(x) = \begin{cases} 0 & x \le S_2 \text{ or } x > S_4 \\ -\dfrac{S_2 - x}{S_3 - S_2} & S_2 < x \le S_3 \\ \dfrac{S_4 - x}{S_4 - S_3} & S_3 < x \le S_4 \end{cases}, \tag{15}$$

$$U_{\mathrm{IV}}(x) = \begin{cases} 0 & x \le S_3 \text{ or } x > S_5 \\ -\dfrac{S_3 - x}{S_4 - S_3} & S_3 < x \le S_4 \\ \dfrac{S_5 - x}{S_5 - S_4} & S_4 < x \le S_5 \end{cases}, \tag{16}$$

$$U_{\mathrm{V}}(x) = \begin{cases} 0 & x < S_4 \\ -\dfrac{S_4 - x}{S_5 - S_4} & S_4 \le x < S_5, \\ 1 & x \ge S_5 \end{cases} \tag{17}$$

where x is the measured value of the relevant factors for the slope to be measured, and S_1–S_5 are the standard values of

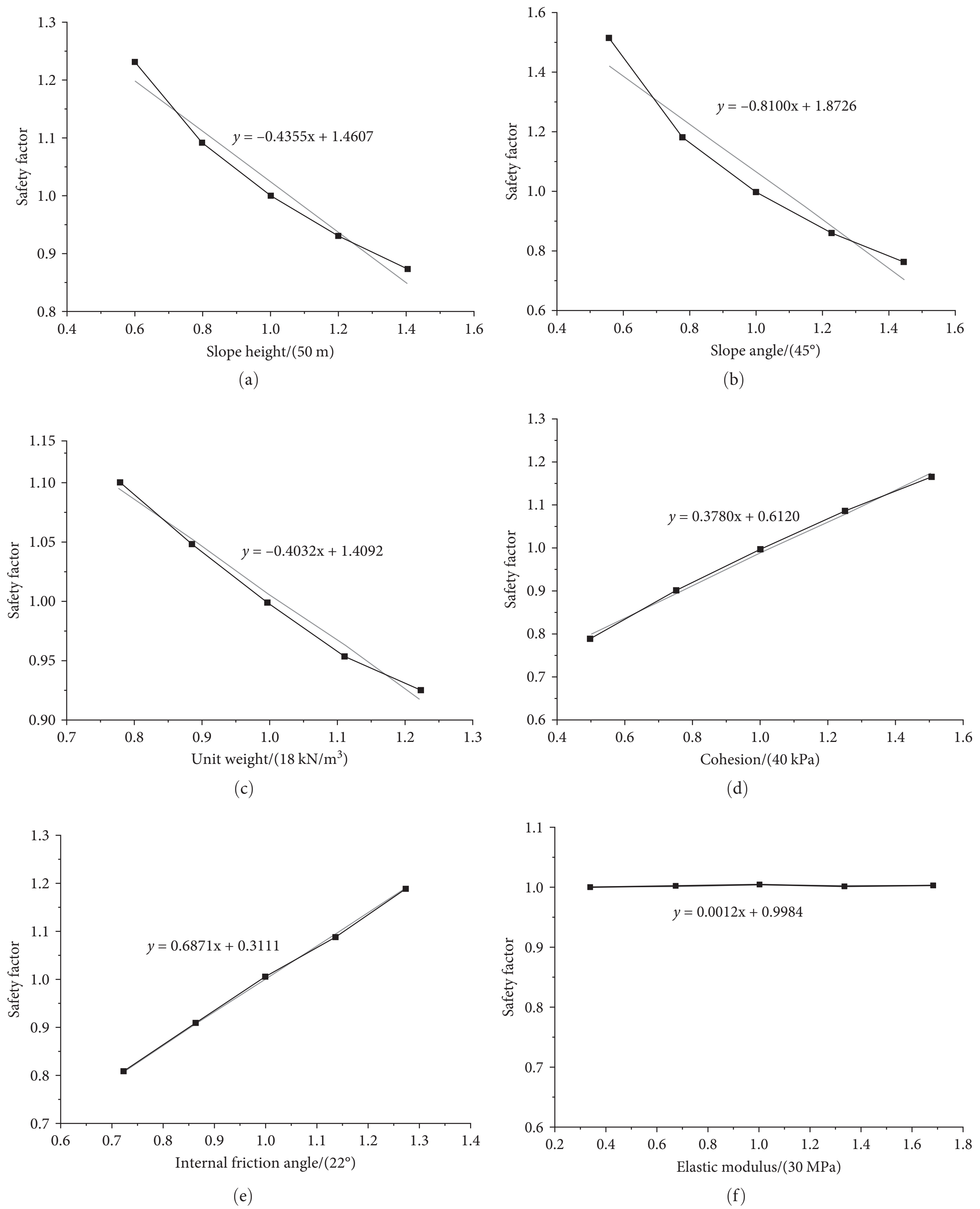

Figure 5: Continued.

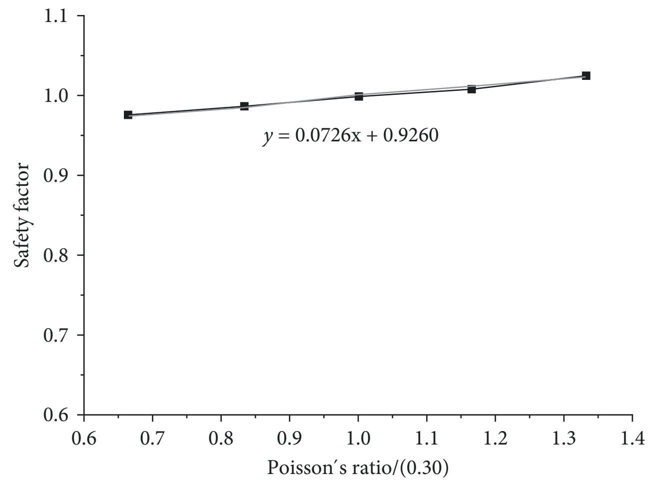

(g)

FIGURE 5: Calculation results of factor sensitivity analysis: (a) relation curve between slope height and safety factor; (b) relation curve between slope angle and safety factor; (c) relation curve between unit weight and safety factor; (d) relation curve between cohesion and safety factor; (e) relation curve between internal friction angle and safety factor; (f) relation curve between elastic modulus and safety factor; (g) relation curve between Poisson's ratio and safety factor.

TABLE 6: Evaluation index stability grading standard.

Index	Evaluation level				
	Stable	Relatively stable	Generally stable	Relatively unstable	Unstable
Slope height (m)	0–6	6–20	20–30	30–90	90–200
Slope angle (°)	0–15	15–30	30–45	45–60	60–90
Unit weight (kN/m^3)	18–30	17–18	16–17	15–16	0–15
Cohesion (kPa)	55–100	40–55	25–40	20–25	0–20
Internal friction angle (°)	35–45	30–35	20–30	15–20	0–15

the evaluation factor that can affect slope stability under five stable conditions.

3.4.3. Determination of Evaluation Index Weight by Gray Correlation Method. The parent sequence and subsequence factors of the loess slope stability evaluation are selected according to the following methods [43, 44]: select the change value of the evaluation index parameters as the subsequence matrix. The values of slope stability coefficient under the condition that one index parameter changes and other parameters fixed were used as the parent sequence matrix [45]. Establish subsequence X and parent sequence Y, as shown in Figure 5(a)–5(e).

$$X = \begin{bmatrix} H \\ \alpha \\ \gamma \\ c \\ \varphi \end{bmatrix} = \begin{bmatrix} 30 & 40 & 50 & 60 & 70 \\ 25 & 35 & 45 & 55 & 65 \\ 14 & 16 & 18 & 20 & 22 \\ 20 & 30 & 40 & 50 & 60 \\ 16 & 19 & 22 & 25 & 28 \end{bmatrix}, \tag{18}$$

$$Y = \begin{bmatrix} 1.23 & 1.091 & 1 & 0.93 & 0.875 \\ 1.508 & 1.177 & 1 & 0.863 & 0.765 \\ 1.102 & 1.048 & 1 & 0.956 & 0.924 \\ 0.793 & 0.898 & 1 & 1.089 & 1.17 \\ 0.809 & 0.907 & 1 & 1.088 & 1.187 \end{bmatrix}. \tag{19}$$

The difference sequence matrix Δ is obtained by range processing of X and Y matrices according to Equations (6)–(8):

$$\Delta = \begin{bmatrix} 1 & 0.358 & 0.148 & 0.595 & 1 \\ 1 & 0.304 & 0.183 & 0.618 & 1 \\ 1 & 0.447 & 0.073 & 0.057 & 1 \\ 0 & 0.029 & 0.049 & 0.035 & 0 \\ 0 & 0.009 & 0.005 & 0.012 & 0 \end{bmatrix}. \tag{20}$$

The gray correlation coefficient matrix L is calculated by Equations (9)–(11) as follows:

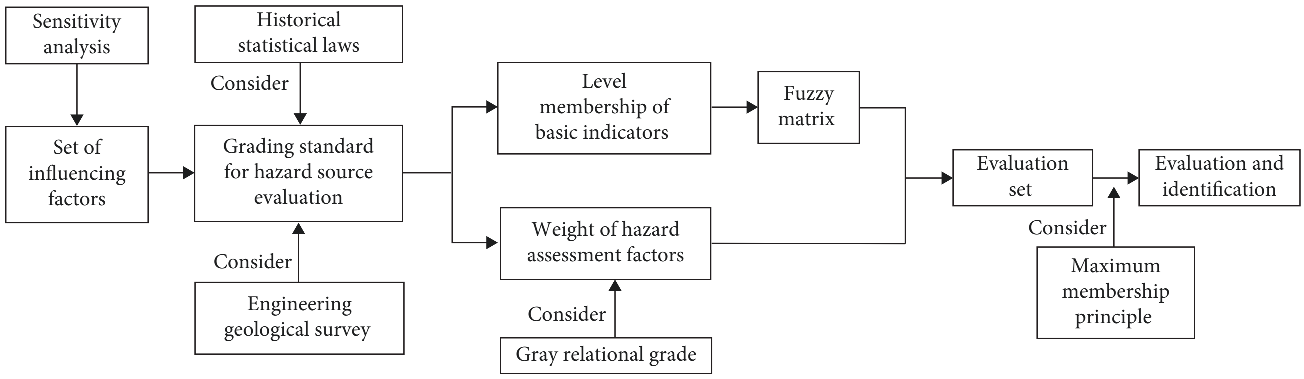

Figure 6: Fuzzy comprehensive evaluation process of loess slope stability.

$$L=\begin{bmatrix}0.333333 & 0.582445 & 0.771739 & 0.456592 & 0.333333\\ 0.333333 & 0.621497 & 0.731299 & 0.447186 & 0.333333\\ 0.333333 & 0.52819 & 0.872549 & 0.467192 & 0.333333\\ 1 & 0.946048 & 0.910628 & 0.934325 & 1\\ 1 & 0.981818 & 0.989529 & 0.976744 & 1\end{bmatrix}. \tag{21}$$

Then, the gray correlation matrix G is calculated by the Equation (10) as follows:

$$\begin{aligned}G&=[H \quad \alpha \quad \gamma \quad c \quad \varphi]^{\mathrm{T}}\\&=[0.378 \quad 0.447 \quad 0.585 \quad 0.826 \quad 1.205]^{\mathrm{T}}.\end{aligned} \tag{22}$$

The weight of each evaluation factor can be obtained by normalizing the gray correlation matrix according to Equation (11) as follows:

$$\begin{aligned}A&=[H \quad \alpha \quad \gamma \quad c \quad \varphi]^{\mathrm{T}}\\&=[0.11 \quad 0.13 \quad 0.17 \quad 0.24 \quad 0.35]^{\mathrm{T}}.\end{aligned} \tag{23}$$

That is, the weight of slope height is 0.11, the weight of slope angle is 0.13, the weight of gravity is 0.17, the weight of cohesion is 0.24, and the weight of internal friction angle is 0.35.

3.5. Fuzzy Comprehensive Evaluation of Slope Stability. As shown in Figure 6, the steps of the fuzzy comprehensive evaluation method for loess slope stability are as follows:

(1) According to the four principles (systematic principle, representativeness principle, operability principle, and hierarchy principle) of evaluation index selection [39], combined with factor statistics and relevant research results of existing literature [46], seven evaluation indexes, namely slope height, slope angle, unit weight, cohesion, internal friction angle, elastic modulus, and Poisson's ratio, are preliminarily selected. Through sensitivity analysis, five evaluation indicators, namely slope height, slope angle, slope unit weight, cohesion, and internal friction angle, are finally selected.

(2) The fuzzy mathematics method was used to establish the membership function of the evaluation index, and the appropriate membership function was selected from the actual value of the evaluation indexes. The corresponding membership degree of each evaluation index to each evaluation grade was calculated. The fuzzy evaluation was made on the basic evaluation index, and the fuzzy relationship matrix R reflecting the fuzzy relationship between U and V is obtained.

$$\boldsymbol{R}=\begin{bmatrix}r_{11} & r_{12} & \cdots & r_{1m}\\ r_{21} & r_{22} & \cdots & r_{2m}\\ \vdots & \vdots & \ddots & \vdots\\ r_{n1} & r_{n2} & \cdots & r_{nm}\end{bmatrix}. \tag{24}$$

In the equation, the nth line reflects the possibility that each factor of the evaluated object takes the nth grade of the evaluation set; the mth column reflects the degree of membership of each grade in the evaluation set corresponding to the mth factor of the evaluated object.

(3) The weight matrix A of the loess slope stability evaluation indexes was obtained by the gray correlation degree method.

(4) Carry out a fuzzy comprehensive evaluation.

$$\boldsymbol{B}=\boldsymbol{A}\cdot\boldsymbol{R}. \tag{25}$$

Note $\boldsymbol{B}=\{b_1, b_2, \cdots, b_m\}$, where b_j reflects the membership of the jth evaluation v_j and fuzzy set B. According to the principle of maximum membership, choose the largest one in B, and the corresponding grade is the final result of the fuzzy comprehensive evaluation.

4. Engineering Application

Based on the design data of Huangyan Expressway, taking into account the statistical data of landslide factors and the existing test results of influencing factors for loess strength, combined with the field survey and reconnaissance, five

Table 7: Parameter value of Yangpoyao slope.

Slope height (m)	Slope angle (°)	Unit weight (kN/m^3)	Cohesion (kPa)	Internal friction angle (°)
25	48	18	21.38	22.93

Table 8: Comparison between fuzzy comprehensive evaluation results of slope stability and field-measured results (From January 2017 to December 2017).

Slope name	Slope type	Stability evaluation grade	Measured cumulative maximum displacement (mm)
Wanhua Tunnel slope	High slope	Relatively stable	34.90
Erlang Mountain slope	High slope	Stable	4.79
Yuetun Reservoir slope	Ancient landslide	Stable	7.94
Yangpoyao slope	High moisture content slope	Generally stable (tend to be relatively unstable)	90.00
Longtou River slope	High slope	Stable	9.84

typical high and steep slopes along the Huangyan Expressway were selected as the research objects of slope stability evaluation, namely the high slope of Wanhua Tunnel, the high slope of Erlang Mountain, the ancient landslide of Yuetun Reservoir, the high water content slope of Yangpoyao, and the high slope of Longtou River.

Taking the Yangpoyao slope with high water content as an example, the fuzzy comprehensive slope stability evaluation was carried out. The value of the evaluation index was obtained according to the aforementioned test data and engineering background information. The strength parameters (mainly including cohesion and internal friction angle) were taken as the cohesion and internal friction angle corresponding to the natural water content of 20.1%. The index value parameters were shown in Table 7.

Determine the membership matrix of the parameter according to the corresponding evaluation index grading standard through Equations (13)–(17) and then calculate the fuzzy relation matrix R as follows:

$$\boldsymbol{R} = \begin{bmatrix} 0 & 0 & 1 & 0 & 0 \\ 0 & 0 & 0.3 & 0.7 & 0 \\ 0.077 & 0.923 & 0 & 0 & 0 \\ 0 & 0 & 0 & 0.91 & 0.09 \\ 0 & 0 & 0.724 & 0.276 & 0 \end{bmatrix}. \tag{26}$$

The weight of each evaluation index was determined by the gray correlation degree method as follows:

$$A = [H \quad \alpha \quad \gamma \quad c \quad \varphi]^{\mathrm{T}} = [0.11 \quad 0.13 \quad 0.17 \quad 0.24 \quad 0.35]^{\mathrm{T}}. \tag{27}$$

Then, perform fuzzy matrix operation according to the following equation as follows:

$$B = A \cdot R = [0.077 \quad 0.17 \quad 0.35 \quad 0.27 \quad 0.09]. \tag{28}$$

According to the principle of maximum membership, choose the largest one max $(b_1, b_2, \cdots, b_m)$ in B, and the corresponding grade was the final result of the fuzzy comprehensive evaluation. When the slope stability evaluation grade is generally stable, the membership degree is 0.35, and when it is relatively unstable, the membership degree is 0.27, which is significantly higher than the corresponding membership degree of other grades. Therefore, the fuzzy comprehensive evaluation results of the stability for the Yangpoyao slope were generally stable but tend to be relatively unstable.

Similarly, the parameter values of the Wanhua Tunnel slope, Yuetun Reservoir slope, Erlang Mountain slope, and Longtou River slope were taken into the stability evaluation model for a fuzzy comprehensive evaluation. The evaluation results are shown in Table 8.

As shown in Table 8, comparing the measured cumulative displacement value of the typical slope with the evaluation grades of slopes stability, it can be seen that the fuzzy comprehensive evaluation results based on the gray correlation degree method are basically consistent with the actual stability of the slopes. Moreover, the evaluation result of the model is in good agreement with the actual situation, which directly indicates that the fuzzy comprehensive evaluation method of loess slope stability based on the gray correlation degree method established in this paper is feasible. It is suggested that the fuzzy comprehensive evaluation method can be popularized in similar projects.

5. Conclusion

Based on literature research, this paper collected and sorted out the geological data of 403 typical landslides and analyzed the slope shape, height, natural slope angle, and rainfall data, providing a data basis for establishing the evaluation method of highway slope stability in loess areas. Then, the finite element numerical calculation method was used to clarify the impact of multiple factors on the stability of loess slopes. Finally, a fuzzy comprehensive evaluation model of slope stability based on the gray correlation degree method was established, and monitoring data verified the evaluation model. The main conclusions are as follows:

(1) The larger the slope angle, the more unstable the slope is. Collapse mainly occurs in the range of 10–40 m slope height, and there is a significant positive correlation between rainfall and the probability of loess landslides.

(2) For the Shaanxi loess slope, the correlation degree (from large to small) between the factors affecting the stability of slopes and the safety factor of the slopes is: slope angle > internal friction angle > slope height > unit weight > cohesion > Poisson's ratio > elastic modulus, and the influence degree of Poisson's ratio and elastic modulus can be ignored.

(3) The fuzzy comprehensive evaluation method based on the gray correlation degree method established in this paper was used to evaluate the stability of the loess slope. The evaluation results are in good agreement with the actual data of slope monitoring. The evaluation method is reasonable and feasible, and can be well applied to the stability analysis of the loess slope.

This paper studied and explored slope stability evaluation in the loess area. At present, slope support, slope reinforcement, and soil permeability are hardly considered in the evaluation grading system. Describing and quantifying the slope support, slope reinforcement, and soil permeability need further in-depth study. The geological environment and climatic environments around the world are very different. Establishing a universal loess slope stability evaluation method is also an important research direction in the future.

Data Availability

Relevant data of this article can be obtained by contacting the corresponding author.

Conflicts of Interest

The authors declare that they have no conflicts of interest to report regarding the present study.

Acknowledgments

The authors are grateful to Dr. Hui Ren for his help with the preparation of figures in this paper. This work was supported by the Science and Technology project of Shanxi Construction Engineering Group (No. 2022-2-12), the Shanxi Water Conservancy Science and Technology Research and Extension Project (No. 2022GM021), and the Shanxi Province University Teaching Reform and Innovation Project (No. J20221260). The financial support is greatly appreciated.

References

[1] J. Zhuang, J. Peng, G. Wang, I. Javed, Y. Wang, and W. Li, "Distribution and characteristics of landslide in Loess Plateau: a case study in Shaanxi province," *Engineering Geology*, vol. 236, pp. 89–96, 2018.

[2] W. Feng, Y. Liu, Z. Chen, Y. Li, and Y. Huang, "Theoretical and practical research into excavation slope protection for agricultural geographical engineering in the Loess Plateau: a case study of China's Yangjuangou catchment," *Journal of Rural Studies*, vol. 93, pp. 309–317, 2022.

[3] J. Peng, P. Sun, O. Igwe, and X"an Li, "Loess caves, a special kind of geo-hazard on loess plateau, northwestern China," *Engineering Geology*, vol. 236, pp. 79–88, 2018.

[4] L. Yurui, Z. Xuanchang, C. Zhi, L. Zhengjia, L. Zhi, and L. Yansui, "Towards the progress of ecological restoration and economic development in China's Loess Plateau and strategy for more sustainable development," *Science of The Total Environment*, vol. 756, Article ID 143676, 2021.

[5] W. Feng and Y. Li, "Measuring the ecological safety effects of land use transitions promoted by land consolidation projects: the case of Yan'an City on the Loess Plateau of China," *Land*, vol. 10, no. 8, Article ID 783, 2021.

[6] J. Zhuang, J. Peng, and Y. Zhu, "Study of the effects of clay content on loess slope failure mode and loess strength," *Bulletin of Engineering Geology and the Environment*, vol. 80, no. 3, pp. 1999–2009, 2021.

[7] X. Li, Y. Lu, X. Zhang, W. Fan, Y. Lu, and W. Pan, "Quantification of macropores of Malan loess and the hydraulic significance on slope stability by X-ray computed tomography," *Environmental Earth Sciences*, vol. 78, no. 16, pp. 1–19, 2019.

[8] P. Xu, H. Qian, Q. Zhang, J. Shang, Y. Guo, and M. Li, "Response mechanism of permeability change of remolded loess to seepage parameters," *Journal of Hydrology*, vol. 612, Article ID 128224, 2022.

[9] P. Xu, H. Qian, S. Li, W. Li, J. Chen, and Y. Liu, "Geochemical evidence of fluoride behavior in loess and its influence on seepage characteristics: an experimental study," *Science of the Total Environment*, vol. 882, Article ID 163564, 2023.

[10] J. Xu, K. Hu, L. Zhou, Y. Li, W. Ye, and S. Wang, "Influence of wet–dry cycles on uniaxial compression behavior of fissured loess," *Environmental Earth Sciences*, vol. 82, no. 1, pp. 1–15, 2023.

[11] J. Zhuang, J. Peng, G. Wang et al., "Prediction of rainfall-induced shallow landslides in the Loess Plateau, Yan'an, China, using the TRIGRS model," *Earth Surface Processes and Landforms*, vol. 42, no. 6, pp. 915–927, 2017.

[12] J. Xu, Z.-Q. Wang, J.-W. Ren, S.-H. Wang, and L. Jin, "Mechanism of slope failure in loess terrains during spring thawing," *Journal of Mountain Science*, vol. 15, no. 4, pp. 845–858, 2018.

[13] Z. Hao, X'an Li, R. Gao, W. Hu, J. Zhang, and J. He, "Experimental study of the effect of bound water on the shear strength and structural units of Malan loess," *Quarterly Journal of Engineering Geology and Hydrogeology*, vol. 56, no. 2, pp. 2021–2168, 2023.

[14] X. Hou, S. K. Vanapalli, and T. Li, "Water infiltration characteristics in loess associated with irrigation activities and its influence on the slope stability in Heifangtai loess highland, China," *Engineering Geology*, vol. 234, pp. 27–37, 2018.

[15] W. Chang, P. Wang, A. Xing, H. Wang, Y. Yu, and X. Li, "Failure mode and dynamic response of loess slopes with tectonic joints under seismic action," *Environmental Earth Sciences*, vol. 80, no. 16, Article ID 531, 2021.

[16] Z.-J. Wu, D.-Y. Zhao, A.-L. Che, D.-W. Chen, and C. Liang, “Dynamic response characteristics and failure mode of slopes on the loess tableland using a shaking-table model test,” *Landslides*, vol. 17, no. 7, pp. 1561–1575, 2020.

[17] X. Zhang, Y. Li, Y. Liu, Y. Huang, Y. Wang, and Z. Lu, “Characteristics and prevention mechanisms of artificial slope instability in the Chinese Loess Plateau,” *CATENA*, vol. 207, Article ID 105621, 2021.

[18] T. K. Raghuvanshi, J. Ibrahim, and D. Ayalew, “Slope stability susceptibility evaluation parameter (SSEP) rating scheme—an approach for landslide hazard zonation,” *Journal of African Earth Sciences*, vol. 99, pp. 595–612, 2014.

[19] C. Yong, D. Jinlong, G. Fei et al., “Review of landslide susceptibility assessment based on knowledge mapping,” *Stochastic Environmental Research and Risk Assessment*, vol. 36, no. 9, pp. 2399–2417, 2022.

[20] K. Tozato, N. L. J. Dolojan, Y. Touge et al., “Limit equilibrium method-based 3D slope stability analysis for wide area considering influence of rainfall,” *Engineering Geology*, vol. 308, Article ID 106808, 2022.

[21] Y.-K. Lee and S. Pietruszczak, “A new discrete form of Hoek–Brown criterion and its application to limit equilibrium analysis of rock slope stability,” *Sustainability*, vol. 14, no. 19, Article ID 12113, 2022.

[22] Z. Su and L. Shao, “A three-dimensional slope stability analysis method based on finite element method stress analysis,” *Engineering Geology*, vol. 280, Article ID 105910, 2021.

[23] Z. Nie, Z. Zhang, and H. Zheng, “Slope stability analysis using convergent strength reduction method,” *Engineering Analysis with Boundary Elements*, vol. 108, pp. 402–410, 2019.

[24] W. Chen, H. Wang, L. Yang, X. Liu, and Y. Chen, “Nonstationary local slope estimation via forward-backward space derivative calculation,” *GEOPHYSICS*, vol. 87, no. 1, pp. 1–11, 2022.

[25] L. Sun, Q. Liu, A. Abdelaziz, X. Tang, and G. Grasselli, “Simulating the entire progressive failure process of rock slopes using the combined finite-discrete element method,” *Computers and Geotechnics*, vol. 141, Article ID 104557, 2022.

[26] F. Zeng, M. N. Amar, A. S. Mohammed, M. R. Motahari, and M. Hasanipanah, “Improving the performance of LSSVM model in predicting the safety factor for circular failure slope through optimization algorithms,” *Engineering with Computers*, vol. 38, pp. 1755–1766, 2022.

[27] L. K. Foong and H. Moayedi, “Slope stability evaluation using neural network optimized by equilibrium optimization and vortex search algorithm,” *Engineering with Computers*, vol. 38, pp. 1269–1283, 2022.

[28] B. Gong, “Study of PLSR-BP model for stability assessment of loess slope based on particle swarm optimization,” *Scientific Reports*, vol. 11, no. 1, pp. 1–10, 2021.

[29] Y. Li, W. Tang, L. Wen, and J. Wang, “Study on seismic failure probability of high earth-rock dam considering dam body deformation and slope stability,” *European Journal of Environmental and Civil Engineering*, vol. 26, no. 9, pp. 3981–3995, 2022.

[30] C. Yin, Z. Wang, and X. Zhao, “Spatial prediction of highway slope disasters based on convolution neural networks,” *Natural Hazards*, vol. 113, no. 2, pp. 813–831, 2022.

[31] R. Yang, J. Huang, and D. V. Griffiths, “Optimal geotechnical site investigations for slope reliability assessment considering measurement errors,” *Engineering Geology*, vol. 297, Article ID 106497, 2022.

[32] L. Sun, B. Zhang, Z. Yin et al., “Assessing the performance of conservation measures for controlling slope runoff and erosion using field scouring experiments,” *Agricultural Water Management*, vol. 259, Article ID 107212, 2022.

[33] A. Yao, Y. Gong, Y. Li, T. Tian, and C. Xu, “Mountain-Expressway Slope Safety Based on the Online Monitoring System and Fuzzy Comprehensive Evaluation,” *Journal of Testing and Evaluation*, vol. 50, no. 4, pp. 1906–1919, 2022.

[34] J. Li, C. Zhao, F. Jia, S. Li, S. Ma, and J. Liang, “Optimization of injection molding process parameters for the lining of IV hydrogen storage cylinder,” *Scientific Reports*, vol. 13, no. 1, pp. 1–15, 2023.

[35] Z. Liu, X. Wang, S. Jia, and B. Mao, “Multi-methods to investigate spatiotemporal variations of nitrogen-nitrate and its risks to human health in China’s largest fresh water lake (Poyang Lake),” *Science of the Total Environment*, vol. 863, Article ID 160975, 2023.

[36] S. Zeng, J. Gu, and X. Peng, “Low-carbon cities comprehensive evaluation method based on Fermatean fuzzy hybrid distance measure and TOPSIS,” *Artificial Intelligence Review*, vol. 56, pp. 8591–8607, 2023.

[37] T. Wan, F. Cheng, Y. Cheng, C. Liao, and Y. Bai, “Investigation into effect of non-uniform thermal environment on thermal sensation under stratum ventilation for heating by using interpolation-based multi-level fuzzy comprehensive evaluation,” *Journal of Building Engineering*, vol. 64, Article ID 105592, 2023.

[38] Y. Zhao, C. Wang, L. Ning, H. Zhao, and J. Bi, “Pore and fracture development in coal under stress conditions based on nuclear magnetic resonance and fractal theory,” *Fuel*, vol. 309, Article ID 122112, 2022.

[39] A. Guo, D. Kong, X. Zhou et al., “Evaluation of material reuse degree in additive manufacturing by the improved resolution coefficient grey correlation method,” *Process Safety and Environmental Protection*, vol. 166, pp. 451–460, 2022.

[40] C. Xu, K. Zhou, X. Xiong, and F. Gao, “Assessment of coal mining land subsidence by using an innovative comprehensive weighted cloud model combined with a PSR conceptual model,” *Environmental Science and Pollution Research*, vol. 29, no. 13, pp. 18665–18679, 2022.

[41] A. K. De, D. Chakraborty, and A. Biswas, “Literature review on type-2 fuzzy set theory,” *Soft Computing*, vol. 26, no. 18, pp. 9049–9068, 2022.

[42] Y. Tang, “Research on risk assessment and monitoring and early warning techniques for Loess Landslides in Northern Shaanxi,” China University of Geosciences (Beijing), (In Chinese), 2012.

[43] G. Tian, H. Zhang, Y. Feng, D. Wang, Y. Peng, and H. Jia, “Green decoration materials selection under interior environment characteristics: a grey-correlation based hybrid MCDM method,” *Renewable and Sustainable Energy Reviews*, vol. 81, pp. 682–692, 2018.

[44] S.-J. Ren, C.-P. Wang, Y. Xiao et al., “Thermal properties of coal during low temperature oxidation using a grey correlation method,” *Fuel*, vol. 260, Article ID 116287, 2020.

[45] H. Chang, W. Shi, W. Li et al., “Experimental optimization of jet self-priming centrifugal pump based on orthogonal design and grey-correlational method,” *Journal of Thermal Science*, vol. 29, no. 1, pp. 241–250, 2020.

[46] C.-L. Gao, S.-C. Li, J. Wang, L.-P. Li, and P. Lin, “The risk assessment of tunnels based on grey correlation and entropy weight method,” *Geotechnical and Geological Engineering*, vol. 36, no. 3, pp. 1621–1631, 2018.